

Influence of Cable Tension on the Mechanical Properties of Cable-stayed Bridge

*Li Xiaozhong and Chen Xingchong**

School of Civil Engineering, Lanzhou Jiaotong University, Lanzhou, 730070, China.

* E-Mail: lj2018576590@163.com

ABSTRACT

The cable force and girder alignment problem of cable-stayed bridge under different damage conditions are studied. According to the characteristics of the force analysis on the cable-stayed bridge, the composite structure composed of cable-stayed cable, main girder and cable tower is considered as an example of a single-tower cable-stayed bridge and the finite element updating model based on the principle of sensitivity analysis is set up with the test data. The cable damage model is established by the elastic modulus reduction method. The effect of single cable and multi-cable force failure on the safety performance of cable-stayed bridge is simulated and the change law of cable internal force redistribution and corresponding deflection caused by different degrees of cable force failure in different position cables is analyzed and summarized. This method provides a basis for damage location and safety assessment of cables of cable-stayed bridges.

KEYWORDS: Cable-stayed bridge, Cable damage, Model updating, Mechanical properties.

INTRODUCTION

The safety of cables as the key structural members of cable-stayed bridges during operation is one of the most important conditions affecting the safety of cable-stayed bridges. The damage of cables will adversely affect the safety, integrity and static and dynamic characteristics of cable-stayed bridges (Shunquan, 2017). Early identification of cable damage and taking timely and necessary measures can effectively avoid adverse effects on cable-stayed bridges and ensure safe operation of bridge structures (Domanescho, 2015; Zhu Jinsong and Xiao Rucheng, 2006). Considering the damage of cables will inevitably lead to the variation and redistribution of cable forces and the variation of cable tension will also reflect in the deflection of bridge deck. How to accurately simulate the cable damage has a great significance to accurately grasp the actual force

condition, the dynamic and static characteristics of the cable-stayed bridge after the cable damage, the distribution law of the cable force and the deflection of the main beam (Brownjohn and Mark William, 2015; Jia, 2016; Jianwei, 2010; Wang, 2010; Yozo, 2002).

Ge Junying and Su Mubiao took a single tower cable-stayed bridge as an example to simulate the broken wire damage of the cable by area reduction method, elastic modulus reduction method, reverse load method and solid element method. The damage of local rusting (unbroken) with different lengths and depths of cables is simulated by the solid element method. The change law of the cable force and the deflection of the main girder after the broken wire damage or local rusting damage of the cable are analyzed (Ge Junying and Su Mubiao, 2016).

In the background of the cable-stayed bridge with twin towers and double cable plane, Zhang Kexin et al. used the spatial finite element model to analyze the damage of the cable and discussed the effect of the cable damage on the deflection and cable force of the cable-

Received on 21/6/2018.

Accepted for Publication on 2/11/2018.

stayed bridge (Sun Quansheng and Zhang Kexin, 2016; Li Yanqiang et al., 2014). Wang Haineng et al. (2014), Li Yanqiang and Zhang Yang (2015) and Dong Xiaoma et al. (2009) studied the establishment process and updating strategy of the benchmark finite element model combined with neural network technology for damage identification. Sun Heng Guang et al. used BP networks to simulate the possible damage location and carried out the reliability analysis considering the attenuation and rupture of cables (Yan Banfu et al., 2017; Sun Zhongguang et al., 2003).

Considering the inhomogeneity of the constitutive behavior of high-strength steel wire and the interaction between steel wires, this paper takes the Silver Beach Bridge as an example to study the effect of cable damage on the mechanical properties of the bridge structure. Based on the tested and measured data of the bridge and

by updating the structural finite element benchmark model, the effect of the cable force failure of single cable and multi-cable on the safety performance of the cable-stayed bridge is simulated and the law of redistribution of the cable internal force caused by the cable force failure is studied.

Engineering Situation

The Silver Beach Bridge is a single-tower and double-cable plane cable-stayed bridge with two spans of 266m (2 x 133m). The cable towers are inverted H reinforced concrete with the height of 79M. The main girder adopts a floating system and 124 main cables are used to connect the main girder with the pylons. From small mileage to large mileage, the cable numbers are S15~S1, 0 and N1~N15. The bridge pattern is shown in Fig.1.



Figure (1): The type of main bridge

Benchmark Model Updating

In order to make the finite element model of ANSYS space to simulate the actual stress state of the main girder and the tower and cable, according to the concrete structure of the bridge, the main girder structure is simulated by the solid element 60002 Shell63. Shell elements are used in the girder body; 484 beam188 units are used in the tower body, link10 unit is used for

simulation in the cable and 62 units in all. At the same time, pavement, railing and deck paving layer only consider the influence of quality when calculating the dynamic characteristics of the structure. The structure of the main bridge is divided into 64642 nodes and 60548 units (Inspection and Test Report, 2005). The finite element model of the full-bridge is shown in Fig. 2.

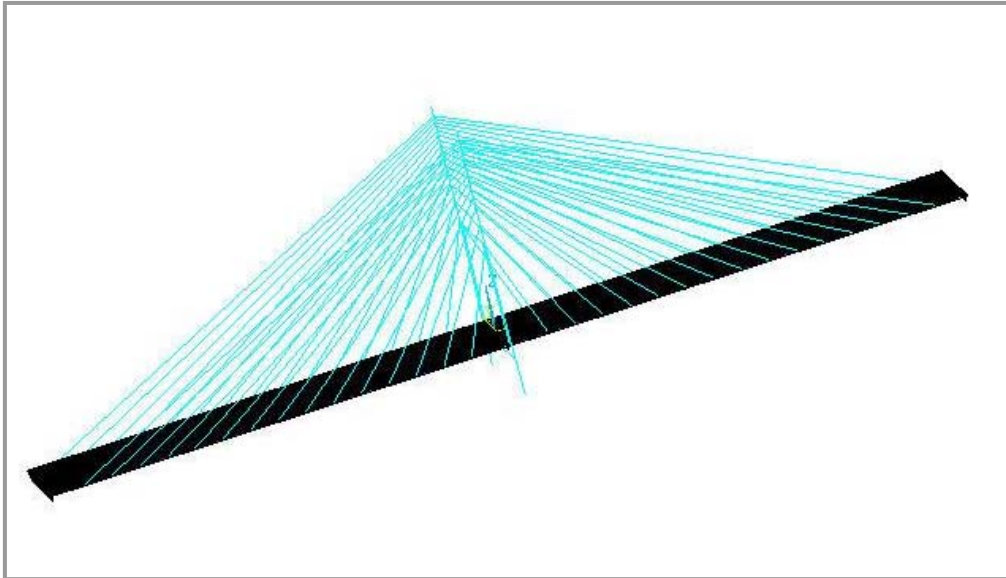


Figure (2): The finite element model of the full-bridge

The finite element model updating is intended to make full use of the relationship between the structural test and finite element analysis and update the finite element model with the data obtained by least structural test in order to obtain the finite element model that is more accurate and close to the structural prototype. The parameter updating method based on sensitivity analysis is an effective updating method (Zheng Rongyue et al., 2006). This paper uses the test data of the cable-stayed bridge and parameter updating method of finite element model based on sensitivity analysis; a modified model is established combined with the result of the bridge dynamic test.

The key of model updating technology based on (modal vector) sensitivity analysis is to represent a real mode as a function of analytical mode, structural parameter and matrix of sensitivity coefficient. Let the real mode be $\{C\}$, which can be expressed as:

$$\{C\} = \{C_0\} + [L](\{P\} - \{P_0\}) \quad (1)$$

where, $\{C_0\}$ is the analytical mode, $[L]$ is the matrix of sensitivity coefficient, $\{P\}$ and $\{P_0\}$ represent iteration and initial parameter vector, respectively. $[L]$ is

the ratio of the change of modal parameters and structural parameters. That is:

$$[L]_{ij} = \frac{\partial C_i}{\partial P_j} \quad (2)$$

where, C_i and P_j represent the i^{th} structural modal parameter and the j^{th} structural parameter, respectively, where $i = 1, 2, \dots, N$ and $j = 1, 2, \dots, M$.

In order to improve the computational efficiency, the sensitivity of the main structural parameters to each mode is first analyzed. Taking the finite element model of the bridge as an example, the analysis and calculation show that the uncertain parameters, which are sensitive to the changes of each order mode, mainly include the elastic modulus and mass density of the concrete structure, the geometric size of the cross-section of the main girder and the crossgirder and the boundary conditions. In the modeling process, the main reasons for the error of the modeling are the crossgirder, the deck pavement, the railings, the cable-stayed web box girder of the cable-stayed bridge, the transition section of the

direct web plate box girder of the cooperative girder and the structural changes after the reconstruction of some structures. The error caused by the nonlinear factors of the material is controlled by processing the elastic modulus and density of the material.

The first 10 modes of vibration and the measured vibration modes and related data obtained from the modified model are shown in Table 1. The correlation between mode shapes and measured modes is calculated and analyzed by modal confirmation criterion (MAC).

$$MAC(\phi_i, \phi_j) = \frac{\left[\{\phi_i\}^T \{\phi_j\} \right]^2}{\left(\{\phi_i\}^T \{\phi_i\} \right) \left(\{\phi_j\}^T \{\phi_j\} \right)} \quad (3)$$

where, $\{\phi_i\}$ and $\{\phi_j\}$ represent the analytical and measured modal vectors, respectively. MAC = 1 means that analysis is completely related to measurement; MAC = 0 means that analysis and measurement are completely irrelevant.

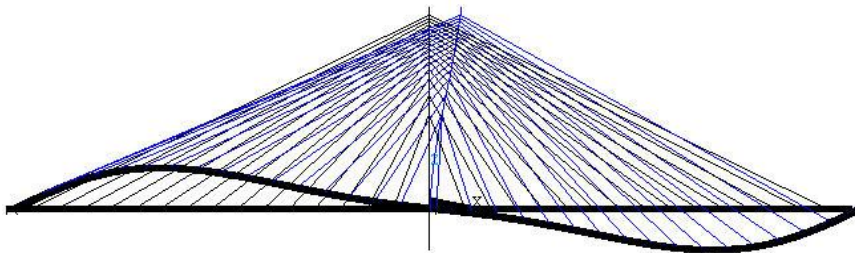
According to the data in Table 1, it is found that the first 10 order frequencies of the modified model are relatively large in addition to the third order (error is 6.61%) and the fourth order (error is 5.15%), while the other errors are relatively small. The MAC values of the updated and measured mode are all above 88%. The updated main vibration mode is shown in Fig. 3, where the vibration mode is well matched with the calculated vibration mode. It can be used as the finite element model of the bridge and the actual state of the structure can be better reflected.

Table 1. Modified and measured mode of the finite element model

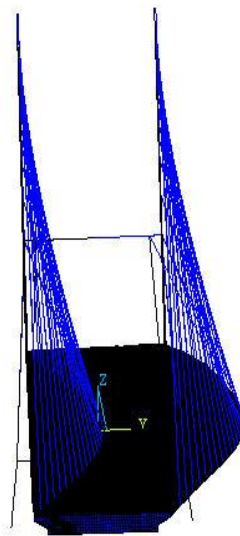
| Modal order | Updated frequency /Hz | M. frequency/Hz | D-value /% | MAC-value/% | Vibration mode |
|-------------|-----------------------|-----------------|------------|-------------|---|
| 1 | 0.491 | 0.488 | 0.61 | 97.3 | Vertical bending |
| 2 | 0.618 | 0.635 | -2.68 | 91.2 | Transverse bending |
| 3 | 0.81 | 0.854 | -5.15 | 89.7 | Tower transverse bending |
| 4 | 0.936 | 0.878 | 6.61 | 90.1 | Vertical bending |
| 5 | 1.129 | 1.172 | -3.67 | 92.8 | Tower transverse bending |
| 6 | 1.328 | 1.366 | -2.78 | 91.6 | Vertical bending and tower longitudinal bending |
| 7 | 1.357 | 1.392 | -2.51 | 88.4 | Beam twist and tower twist |
| 8 | 1.475 | 1.513 | -2.51 | 92.4 | Girder bending |
| 9 | 1.89 | 1.879 | 0.59 | 93.5 | Beam twist and tower transverse bending |
| 10 | 1.96 | 1.95 | 0.51 | 89.6 | Girder vertical bending |



(a) The first vibration mode of the main bridge



(b) The second vibration mode of the main bridge



(c) The third vibration mode of the main bridge

Figure (3): Vibration modes of the main bridge

Damage Analysis of the Cable

On the basis of the modified benchmark model, the damage degree and distribution of the cables are simulated and the distribution of girder alignment and cable force under various damage conditions is calculated.

Cable Damage Simulation

The stress distribution of steel wire inside the cable is uniform, which is composed of multiple parallel steel hinges and is subjected to a single axial force; the damaged cables and their nearby cables are all in the elastic working state. If the damage of cables is due to the change of stiffness coefficient of the cables, the elastic modulus reduction method is better (Ge Junying and Su Mubiao, 2016).

A one-dimensional fiber bundle model in damage theory is introduced to further characterize its damage characteristics. As shown in Fig. 4, it is assumed that the fiber bundle is made up of a large number of parallels, same length fibers and the root fibers are independent to each other; that is, there is no lateral interaction force. The mechanical properties of fiber bundles, such as strength and stiffness, depend entirely on the nature of each fiber. This is consistent with the composition of the parallel wire in the cable-stayed cable. If the Young's modulus of each parallel steel wire is the same, the stress of the cable will be the same as:

$$\sigma^* = \frac{F}{A(1-c)} \tag{4}$$

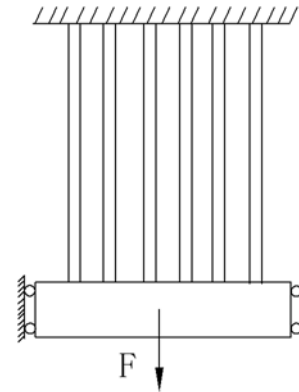


Figure (4): One-dimensional fiber bundle model

The formula is in the same form as the effective stress defined by Kachanov. The physical meaning of $1 - c$ in the fiber bundle model is the ratio of the cross-section area of the remaining fiber to the cross-section area of all fibers, which is equivalent to the continuity φ in the Kachanov damage model and c is a direct measure of the fiber bundle damage, which is equivalent to the damage factor ω in Rabotnov damage model. When the damage occurs, the strength and service performance of the cable are determined by the effective bearing area \tilde{A} of the cable and the whole section of the cable is regarded as a continuous medium. The damage rate ω is defined as the ratio of the cross-section area $(A - \tilde{A})$ of the broken steel hinge line to the cross-section area A of the original steel reaming line; i.e., $\omega = (A - \tilde{A}) / A = 1 - \tilde{A} / A$. Therefore, the damaged cable can be expressed by the reduction of the elastic modulus in the finite element calculation and the elastic modulus is $E(\omega) = (1 - \omega)E$. In this paper, the damage rate of cables is equal to 40%, 60% and 80%, compared with the breaking condition ($\omega=100\%$) and the intact state ($\omega=0$). The elastic modulus corresponding to different cable damage degrees is shown in Table 2.

Table 2. The elastic modulus corresponding to different damages of cables

| ω | 0 | 40% | 60% | 80% | 100% |
|--------------------|----------------------|----------------------|----------------------|----------------------|------|
| $E(\omega)(N/m^2)$ | 2.0×10^{11} | 0.8×10^{11} | 1.2×10^{11} | 1.6×10^{11} | 0 |

Alignment Shape Analysis of Main Girder under Different Cable Damage

First, the influence of cable damage along the longitudinal direction of bridge deck on the alignment of main girder is discussed. In order to facilitate the analysis and set clearer rules, three cases are assumed to the cross-section of the cable; namely, the cable is broken along the side of the cross-section, completely symmetric breaking and asymmetric breaking; that are symmetrical breaking in the midspan, symmetry to the axis of the bridge and asymmetric breaking. In the three cases, the results are shown in Figs. 5- 9.

It can be seen that: (1) In Fig.5, S4 and S8 are broken, the line shape of the main girder is obvious near the inner broken alignment of the main beam and the main tower has no influence on the alignment of the main girder; the broken area of S12, S14 and S15 appears in the upper arch and the lower arch appears in the other side of the main tower, where the amplitude of the upper and lower arches is $S15 > S14 > S12$. The upstream and downstream of cable 0 are broken, except the influence on the main girder alignment in area N3-S3; the alignments in other areas are almost identical to the alignment shape of the main girder; that is, the breaking of S0 is only influenced by the anchorage points of the

main girder from N3-S3. (2) It can be seen from Fig. 6 that the main girder alignment is symmetrical at 0 coordinate towers and the two sides are symmetrical under the deflection alignment. The breaking of each cable has great influence on the ride comfort of the main girder deck. Taking S0 breaking as an example, there is a clear reverse point in the midspan. (3) From Figs. 7-9, it can be seen that the maximum deflection of S0, S4 and S8 breaking appears on the breaking side with a slight distortion of the main girder. S14 and S15 breaking causes the line to appear in the upper arch on the breaking side, while on the opposite side of the tower a big lower arch appears (the lower arch is the biggest when S15 breaks) and the main girder is distorted.

The damage of cables in different degrees is simulated numerically in Table 2. The influence of the different degrees of damage of the outermost cable S15 on the girder alignment is shown in Table 3 and Fig.10. It can be seen from the diagram that: taking S15 as an example, the downwarp on the damage side appears when the damage degree is 20% and 40%; the upper arch gradually appears under the damage degree of 60%, 80% and 100%. However, on the other side of the tower, the increment of downwarp accelerates with the increase of damage.

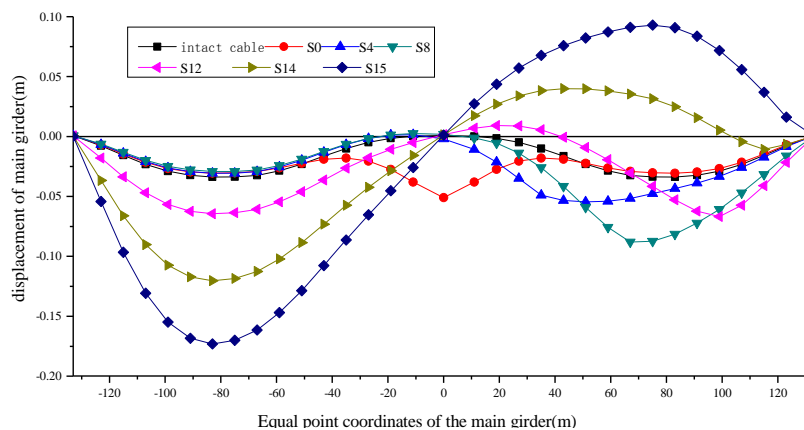


Figure (5): The displacement diagram of breaking main beam with single symmetry

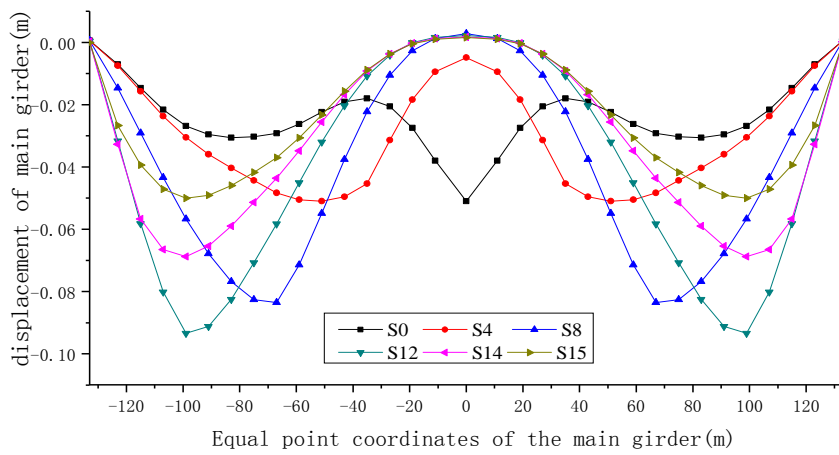


Figure (6): The displacement diagram of breaking main beam with double symmetry

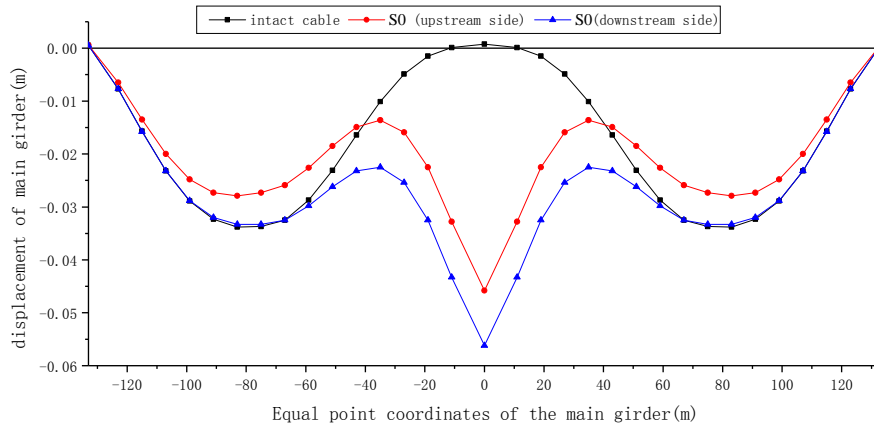


Figure (7): The influence of the downstream side breaking of S0 cable on the line shape of the main girder

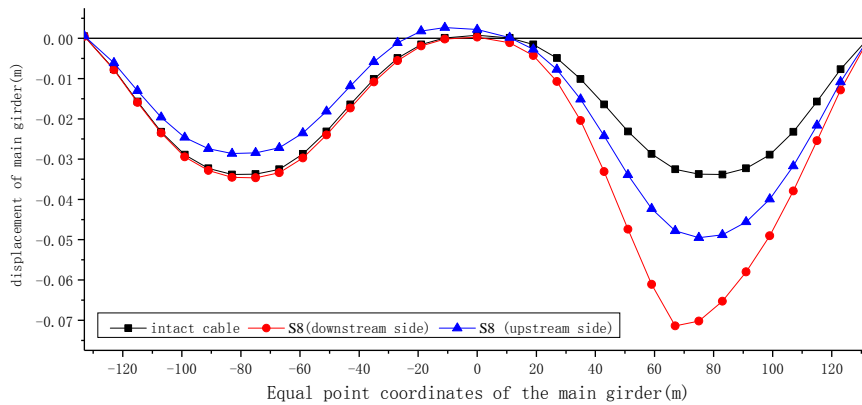


Figure (8): The influence of the downstream side breaking of S8 cable on the line shape of the main girder

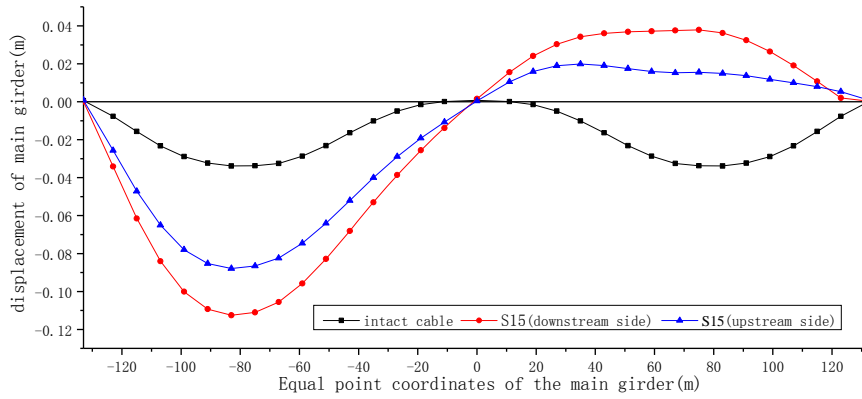


Figure (9): The influence of the downstream breaking of S15 cable on the alignment shape of the main girder

Table 3. Description of different damage degrees of S15 and increment of mid-span deflection

| Working condition | Working condition description |
|-------------------|---------------------------------------|
| S15-40% | The damage degree of cable S15 is 40% |
| S15-60% | The damage degree of cable S15 is 60% |
| S15-80% | The damage degree of cable S15 is 80% |
| S15-100% | The breaking of cable S15 |

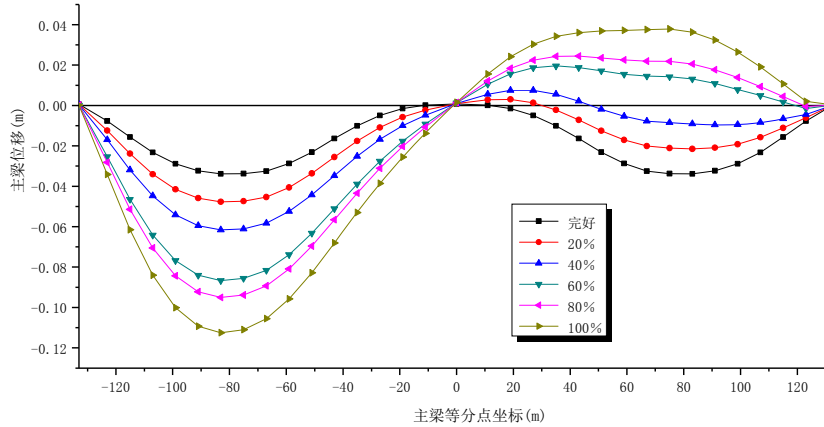


Figure (10): Influence of the upstream damages of S15 on the girder alignment

Cable Force Analysis under Different Damage Degrees of the Cable

The influence of cable damage on the main bridge is

similar to that of cable tension under different degrees of damage. In the limited space, the cable tension distribution law is summed up by the representative

cable tension amplitude. The definition of cable force amplitude is shown in Equation 5 and the analysis results are shown in Figs. 11-13.

$$\delta f = \frac{N^d - N^u}{N^u} \times 100\% \quad (5)$$

in which N^d and N^u are the damaged and undamaged cable force, respectively and δf denotes the cable force amplitude.

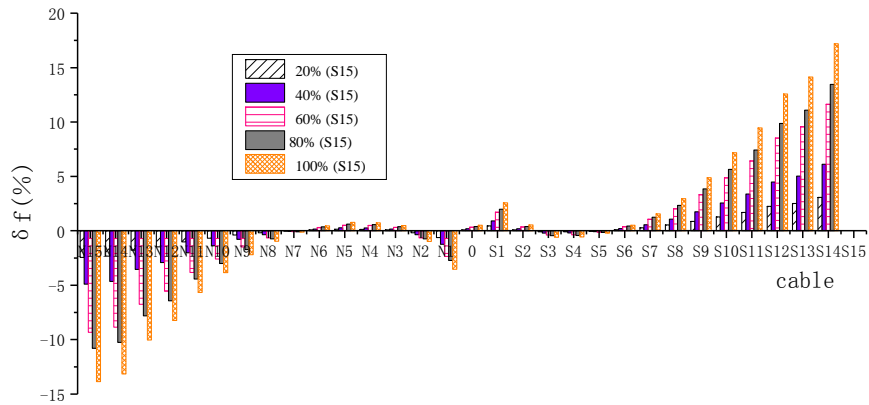


Figure (11): The influence of different damage degrees of S15 on other cable forces

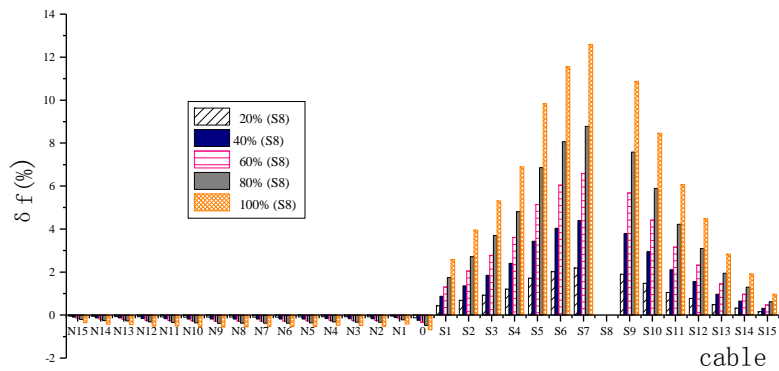


Figure (12): The influence of different damage degrees of S8 on other cable forces

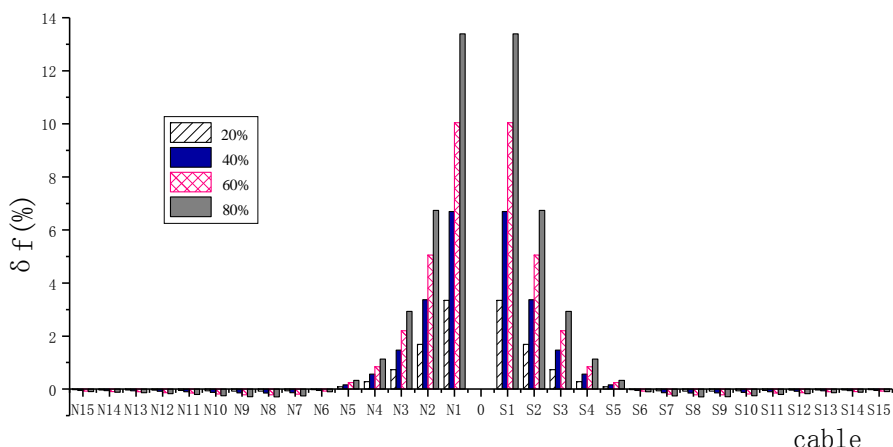


Figure (13): The influence of different damage degrees of cable 0 on other cable forces

It can be seen from the diagrams that: (1) In Fig. 11, under different degrees of damage of S15, the amplitude of cable force shows an antisymmetric characteristic and the amplitude of cable force increases regularly with the increase of damage. When the damage degree reaches 80%, the cable force amplitude over 5% is S10 to S14, N11 to N15. (2) In Fig. 12, under different degrees of damage of S8, the cable force amplitude is mainly concentrated on the damage side, while the opposite side is not significant; meanwhile, the cable force amplitude decreases at both sides with S8 as the center. When the damage degree reaches 80%, the cable force amplitude exceeding 5% is S5, S6, S7, S9 and S10. (3) In Fig.13, under different degrees of damage of cable No. 0, the cable force amplitude is mainly concentrated on both sides of cable 0. When the damage degree reaches 80%, the cable force amplitude exceeding 5% is N2, N1, S1 and S2.

CONCLUSIONS

In this paper, a cable-stayed bridge is taken as the research object. Through the modified model system, the change law of the line shape and cable force of the main girder is discussed under different damage conditions of the cable. The conclusions are as follows:

- (1) Combining the stress characteristics of cable-stayed bridge and the measured data, the updating method based on the finite element model based on sensitivity analysis is feasible and the effect of elastic modulus reduction for cable damage is better.
- (2) When the cable close to the cable tower breaks, the downwarp line near the main girder is obvious and the opposite side has no obvious change. However, the closer to the back cable breaking, there will be regular arch phenomenon in the opposite side of the tower. Asymmetrical breaking will result in the distortion of the main girder line.
- (3) When the cable is damaged to different degrees, the girder alignment of the damage zone is gradually decreasing and the opposite side of the cable tower appears in upward arch gradual change. At this time, the amplitude of the cable force S15 exhibits the characteristics of antisymmetry. Cable S0 shows symmetrical distribution on both sides and S8 mainly concentrates on the damage side and has little effect on the opposite side.

Acknowledgement

This work is supported by the National Natural Science Foundation of China (No.51468031 and 51768037).

REFERENCES

- Brownjohn, James, and Mark William. (2018). "Bayesian operational modal analysis of Jiangyin Yangtze River Bridge". *Mechanical Systems and Signal Processing*, 110, 210-230.
- Domaneschi, Marco. (2015). "Damage detection and localization on a benchmark cable-stayed bridge".
- Dong Xiaoma, Sun Qingzhen, and Li Guanghui. (2009). "Research on cable damage identification of cable-stayed bridges based on modal strain energy index". *Engineering Journal of Wuhan University (Engineering Edition)*, 42 (6), 785-788.
- Ge Junying, and Su Mubiao. (2016). "Simulation method for cable damage of cable-stayed bridge and its effect on cable tension and deflection distribution". *China Railway Science*, 37 (03), 30-37.
- Inspection and Test Report on the Silver Beach of Yellow River Bridge. (2005). Lanzhou Jiaotong University.
- Jia, Buyu. (2016). "Study on the system reliability of steel-concrete composite beam cable-stayed bridge". *Open Civil Engineering Journal*, 10, 418-432.
- Jianwei Li. (2010). "Static and dynamic analysis and test of cable-stayed bridge with cable damage". Northeast Forestry University.
- Li Shunlong. (2014). "SMC structural health monitoring benchmark problem using monitored data from an actual cable-stayed bridge".
- Li Xiaozhong. (2007). "Influence of cable tension on the mechanical properties of cable-stayed bridge". Lanzhou Jiaotong University.
- Li Yanqiang, and Zhang Yang. (2015). "Step-by-step damage detection for cable-stayed bridge based on support vector machine and hierarchic genetic algorithm". *Earthquake Engineering and Engineering Dynamics*, 35 (6), 71-77.
- Li Yanqiang, Zhao Shiyang, and Du Yanliang. (2014). "Damage identification method for the main girder of cable-stayed bridge based on the tension indices of the most sensitive stay cable". *China Railway Science*, 35 (2), 20-25.
- Qin Shunquan. (2017). "Developments and prospects of long-span high-speed railway bridge technologies in China". *Bridge Engineering and Tunnel Engineering*, 3 (6), 787-794.
- Sun Quansheng, and Zhang Kexin. (2016). "The impact analysis of cable damage on the static performance of cable-stayed bridge". *Highway Engineering*, 41 (3), 35-39.
- Sun Zhongguang, Ni Yiqing, Gao Zanming, and Ding Haojiang. (2003). "Damage locating of cable-stayed bridges based on dynamic measurement and neural network technique". *Engineering Mechanics*, (3), 26-30.
- Wang Haineng, Liu Jie, Wang Xinmin, and Zhang Zhiguo. (2014). "A new method and implementation of establishing a benchmark finite element model for cable-stayed bridges". *Journal of Vibration, Measurement and Diagnosis*, 34 (3), 458-462+588.
- Wang Jinzhao. (2010). "Theoretical analysis and health monitoring method for cable breaking risk of long-span cable-stayed bridges". Northeast Forestry University.
- Yan Banfu, Sun Yanfeng, and Zou Qiqi. (2017). "System reliability analysis on the cable-stayed bridge considering cable breakage and resistance degradation". *Journal of Hunan University (Natural Sciences)*, 44 (9), 10-16+40.
- Yozo Fujino. (2002). "Vibration control and monitoring of long-span bridges-recent research, developments and practice in Japan". *Journal of Constructional Steel Research*, 58, 71-97.
- Zheng Rongyue, Lv Zhongda, Xu Kaiming et al. (2006). "Dynamic analysis of Ningbo Baoshan Bridge based on model updating". *Journal of Highway and Transportation Research and Development*, 23 (5), 52-56.
- Zhu Jinsong, and Xiao Rucheng. (2006). "A study on the safety assessment method for stay cables of long-span cable-stayed bridges".